UC Irvine
UC Irvine Previously Published Works

Title

The role of primary jet injection on mixing in gas turbine combustion

Permalink

https://escholarship.org/uc/item/2dh8h042

Journal

Symposium (International) on Combustion, 23(1)

ISSN

0082-0784

Authors

Richards, CD
Samuelsen, GS

Publication Date

1991

DOI

10.1016/s0082-0784(06)80366-8

Peer reviewed

THE ROLE OF PRIMARY JET INJECTION ON MIXING
IN GAS TURBINE COMBUSTION

C. D. RICHARDS AND G. S. SAMUELSEN

UCI Combustion Laboratory
Institute of Combustion and Propulsion Science and Technology
University of California
Irvine, CA 92717

The role of primary jet injection on the aerothermal structure and overall performance of a model gas turbine combustor is addressed in an experimental study. The impact of momentum ratio between the primary jets and the swirl air as well as the relative position of the jet row to the swirler injection plane are investigated in a combustor operated on propane at atmospheric pressure. The aerodynamic and thermal fields are characterized using laser anemometry and a thermocouple probe respectively. Species concentrations are acquired at the exit plane via extractive probe sampling. Four regimes are identified that describe the degree of interaction of the primary jets with the swirl-induced recirculation zone. For each regime, the degree of jet penetration and entrainment in the recirculation zone and, as a result, the aerothermal structure of the dome region are substantially different.

Introduction

The design of gas turbine combustors is today predicated on empirical data associated with the overall combustion performance of the system. Although experimental research has been conducted in both laboratory bench scale and full scale hardware,[1-5] little is yet understood about the detailed aerodynamics, the detailed mixing of fuel and air, and the relationship of these processes to the overall system performance. For example, although the primary jets are known to play an important, and perhaps dominant role, in the mixing processes within the combustor (jet penetration, interaction with the swirl-induced recirculation zone, provision of air to both the dome and intermediate zone), no in-situ information is available on the detailed effect of primary jet interaction with the aerothermal structure of the combustor.

In this paper, the role of the primary jets in affecting the dome region aerodynamics, the temperature field, and the emission of gaseous products is addressed. A model laboratory can combustor is employed with (1) optical access and (2) the essential features of gas turbine combustors including spray injection, swirl-stabilized dome aerodynamics, and wall jet injection. Laser anemometry (LA), a thermocouple probe, and a gas extractive probe are used for documenting the aerodynamic and thermal fields, and gaseous emissions respectively. In addition to providing physical insight, data are acquired for use in the development and evaluation of numerical codes destined for industrial combustor design.

Background

The combustors used in this study are based on a model combustor dubbed the Wall Jet Can Combustor, WJCC.[6] This combustor, shown schematically in Fig. 1a, features dome swirl and two rows of discrete wall jets. Each row of jets consists of four individual jets with an injection angle of 90 degrees.

The basic performance of this combustor has been characterized via detailed spatial maps of velocity, temperature, and droplet field statistics, and found to produce an overall flowfield and combustor performance considered to be representative of a practical gas turbine combustor.[6,7]

In the previous studies, the combustor was a double-walled, water cooled stainless steel duct with two opposing windows for optical access along the length of the combustor. The combustor modules employed in the present study feature the same general characteristics—namely, dome swirl and two rows of discrete wall jets—but are fabricated from quartz to provide unrestricted optical access from wall to wall for the purposes of facilitating the application of visualization diagnostics. Several modules were manufactured so that a parametric variation of the number of jets per row and axial position of the jets could be performed.

In a recent study,[8] the interaction of the opposed radial jets with a swirl-induced recirculation zone was explored in these modules under isothermal conditions. In each case, the jet-to-crossflow momentum ratio (G_r) and relative position of the jet row to the swirler injection plane were varied. Four regimes were selected to characterize the flowfield structure. In Regime I, the momentum ratio (G_r) is very low and the jets are (1) deflected into a spiral trajectory, and (2) remain close to the wall.[8,9] The recirculation zone is long and can extend out the exit of the combustor. In Regime II, the jets are deflected sufficiently by the swirling crossflow to preclude penetration to the centerline but have, nonetheless, a substantial influence on the structure of the recirculation zone. In particular, the recirculation zone is considerably shortened (compared to Regime I). The axial extent of the recirculation zone is dependent on G_r. In Regime III, G_r is higher, and although the jets are still deflected by the swirling crossflow, the jet momentum is sufficient to penetrate to the centerline downstream. The downstream axial distance required for penetration is dependent upon G_r. For Regime IV, the momentum ratio is sufficiently high to induce jet penetration to the centerline with virtually no axial deflection, and to produce a backflow which feeds into the recirculation zone.

In this study, the effect of jet-to-swirl momen-

tum ratio is investigated for a reacting condition. The goal is to identify the impact of momentum ratio on the combustor performance in general, and the aerodynamic and thermal fields, and emission of gaseous species in particular.

Experiment

Approach:

The approach was to detail the aerodynamic and thermal fields of the combustor and gaseous emissions at the exit plane for two modules and a variety of jet-to-crossflow momentum ratios (G_r). Measurements of velocity were made across the radius of the combustor in increments of 4 mm at selected axial locations as well as along the centerline. A thermocouple probe was used to obtain the average temperature across the radius in 4 mm increments at 11 axial locations. An extractive probe and gas analyzers were used to determine species concentrations at an axial location 2.5 duct diameters downstream of the nozzle inlet plane.

Test Bed:

The combustor modules, patterned after the WJCC, are 80 mm quartz ducts with an operating length of 32 cm (Fig. 1a). Air flow to the combustor

a) The Wall Jet Can Combustor (WJCC).

b) Measurement planes.

Plane between jets. (velocity, temperature) Plane through jets. (temperature) Exit plane. (emissions)
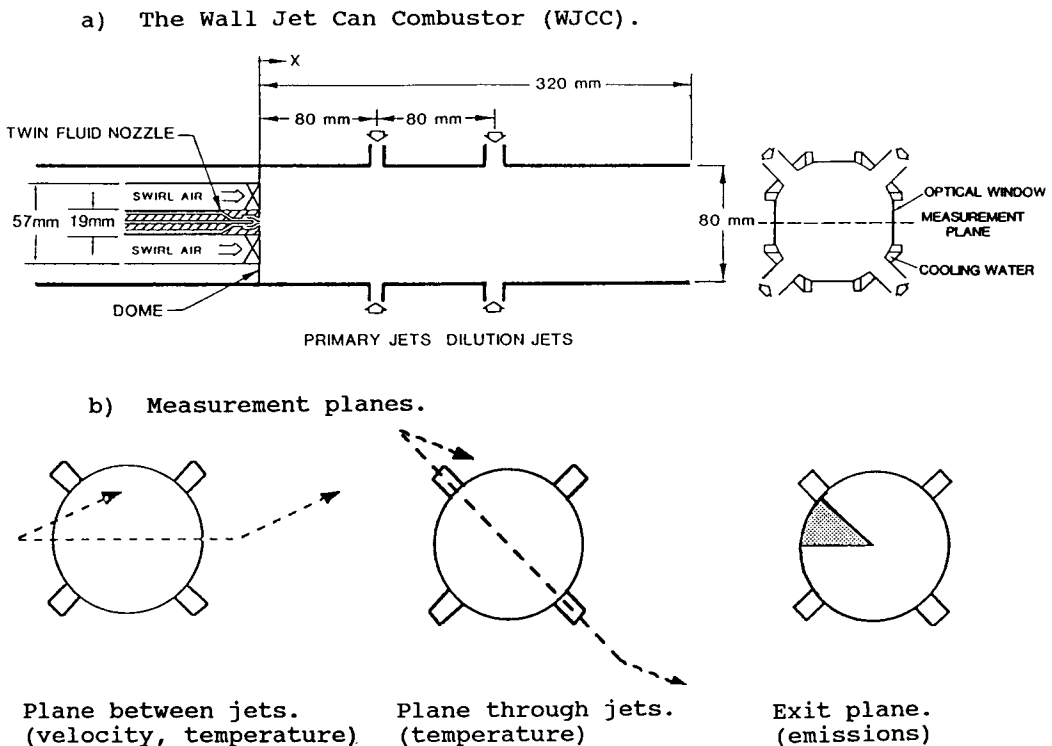
FIG. 1. The model combustor geometry.

is split into three separate lines: dome swirl, primary jets, and dilution jets. Each line is separately metered and controlled so that the flow splits may be varied. The swirl air enters the combustor at the inlet plane through a 34 mm diameter, 100% blockage, 45 degree swirler. Each of the wall jet lines are further split into 4 lines which (1) feed the discrete wall jets, and (2) are individually controlled and metered, an essential requirement to assure symmetric flow within the combustor.

A 19 mm O.D. centrally positioned fuel delivery assembly is sized to house a cone annular (70 degree full angle) gaseous fuel nozzle. The dome swirl vanes are concentrically positioned around the fuel delivery assembly as shown in Fig. 1a.

Each combustor module features two rows of discrete wall jets, a primary jet row and a dilution jet row. The axial position of the jet rows varies between the modules. Module 1, the baseline case, consists of 4 jets per row positioned one and two duct diameters downstream from the inlet. Module 2 also features 4 jets per row but they are positioned 1/2 and 3/2 duct diameters downstream from the inlet. The diameters of the primary jets and dilution jets in both cases are 7.5 and 10 mm respectively.

Diagnostics:

A single component laser anemometer (LA) system, described in detail elsewhere,[1] was used to characterize the flowfield velocities. Measurements of mean and rms axial velocities were acquired in the plane of symmetry between the jets as shown in Fig. 1b.

The thermal field was established using a Type R thermocouple probe mounted on a three-axis positioning traverse. The data are presented uncorrected for radiation loss. Temperature measurements were obtained in the plane of symmetry between the jets as well as in the plane of symmetry through the jets as shown in Fig. 1b.

Exit plane species concentrations were determined with a water-cooled extractive probe mounted on a three axis positioning traverse. Concentrations of oxygen, carbon dioxide, carbon monoxide, nitric oxide, and nitrogen dioxide were acquired using a Beckman Model 755 O_2 analyzer, Horiba PIR 2000 analyzers for CO and CO_2, and a TECO Model 10 analyzer for NO_x concentrations. Species concentrations were obtained at an axial plane 2.5 duct diameters downstream of the inlet plane in a slice defined by the two planes of symmetry as shown in Fig. 1b. The axial plane was selected to be near the end but within the combustor duct.

Test Conditions:

Flowrates to the swirler and primary jets were identical to those in the isothermal study.[8] Al-

though the dilution jet flow is important to the exit temperature profile and emission pattern, the objective of this study was focused on the role of the primary jets. The dilution flow was, as a result, maintained at a constant level.

The fuel, propane, was injected at a flowrate of 3.13 kg/hr and 3.76 kg/hr in Module 1 and Module 2 respectively. Based on the swirl air alone, this provided equivalence ratios of 1 and 1.2 respectively in the dome region. An enriched dome was necessary to sustain a stable reaction at the higher primary jet flows in Module 2.

The mass flow through the swirler was kept constant at 40.3 kg/hr and the primary jet mass flow was varied to produce momentum flux ratios, G_r in the range of 1.74 to 6.99. The flowrates and momentum ratios are presented in Table I along with the definition for G_r.

Results And Discussion

Aerodynamic Field:

Centerline mean axial velocity profiles acquired in Module 1 are shown in Fig. 2a for three jet-to-crossflow momentum ratios (G_r). (The positions of the primary and dilution jets are marked by arrows on the plot; "x_o," denotes the position of the primary jet row.) The centerline mean axial velocity, U_{cl}, has been added to and normalized by $V_j/2$ (V_j is the primary jet velocity) to form the vertical axis. When this quantity is unity, U_{cl} is zero (i.e., the stagnation point where the jets meet). This gives an indication of the degree of penetration and strength of the jets.

For $G_r = 1.74$ the centerline velocities are negative until just downstream of the primary jets. Visualization of the flow at this condition reveals that the primary jet trajectories are deflected, and the jets do not penetrate to the centerline. This is an example of Regime II.

As the momentum flux of the jets is increased to 3.93, (1) the jets are deflected less, and (2) the up-

Table 1

Flow conditions and momentum ratios.

A_j/A_s	m_j[a] kg/s	V_j/V_s	G_r[b]
0.283	1.98×10^{-3}	2.48	1.74
0.283	2.97	3.72	3.93
0.283	3.96	4.96	6.99

a. m_j is the mass flow through one primary jet.
b. $G_r = A_j/A_s(V_j/V_s)^2$, where V_s is based on the bulk mass flow rate to the swirler, the swirl angle, and the swirler inlet area, A_s.
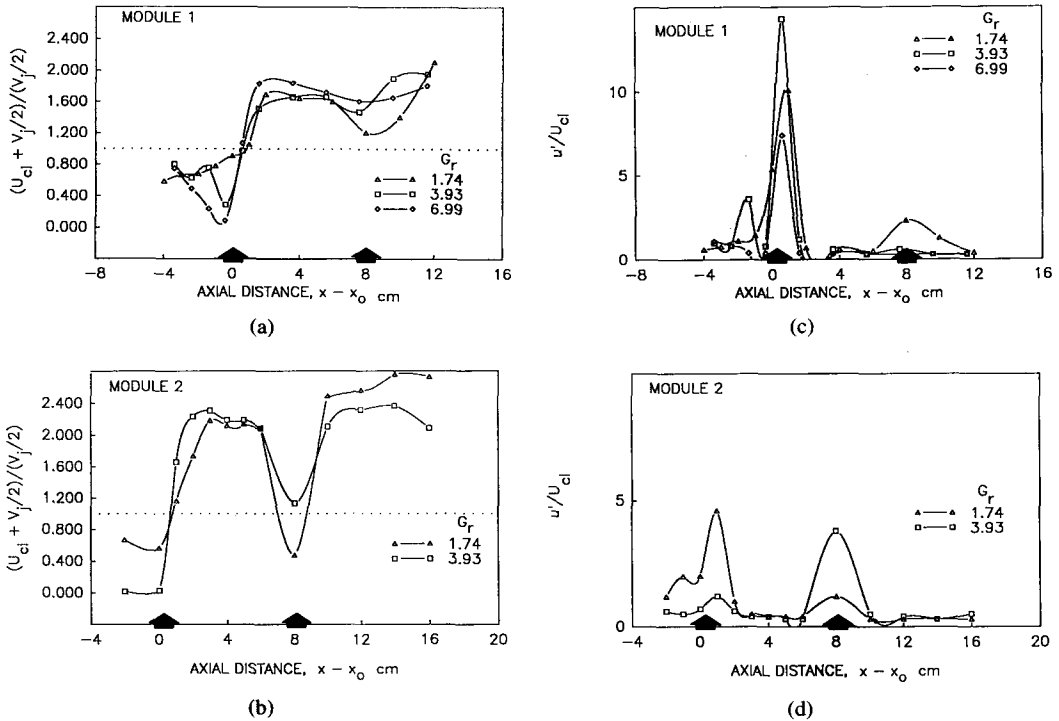
FIG. 2. Centerline mean and rms velocity.
a) Centerline mean axial velocity profiles in Module 1 for a variation in G_r.
b) Centerline mean axial velocity profiles in Module 2 for a variation in G_r.
c) Centerline axial turbulence intensity profiles in Module 1 for a variation in G_r.
d) Centerline axial turbulence intensity profiles in Module 2 for a variation in G_r.

stream mass flux into the dome is enhanced as reflected by the increased negative velocities. Two regions of backflow occur, one associated with the recirculation zone and one with the penetration and subsequent splitting of the jets. The local maximum at $x - x_o = -2$ cm is the interface. This is characteristic of Regime III.

At $G_r = 6.99$ (Regime IV), it is not possible to distinguish the contribution from the recirculation zone from that of the swirl air and that of the jet contribution. At this point, the jets feed directly into the recirculation zone.

In Fig. 2b, profiles of centerline velocity are shown for Module 2. At both momentum ratios, the flow is in Regime IV. The placement of the jets abruptly and effectively destroys the evolution of the swirl-induced recirculation zone, thereby allowing the jet flow to penetrate to the centerline. Note that the destruction of the swirl allows, as well, the dilution jets to avoid deflection and penetrate to the centerline.

In Fig. 2c, plots of turbulence intensity (with the rms velocity normalized by the local centerline velocity, U_{cl}) are presented. Clearly defined peaks occur at locations corresponding to jet penetration for

all cases. For $G_r = 1.74$, the region of elevated turbulence intensity monotonically increases and decreases from $x - x_o = -1$ to 2 cm whereas, for $G_r = 3.93$, two clearly defined peaks occur at $x - x_o = -1.5$ and 1 cm respectively. For the highest momentum ratio (6.99), only one peak is revealed.

The difference in these patterns may be explained by evaluating the manner by which the jets penetrate the crossflow. For the smallest momentum ratio (1.74), centerline velocity plots show that flow reversal ends at approximately $x - x_o = 1$ cm. All velocities are positive downstream from this point. For $G_r = 3.93$, velocities are negative upstream of this point to approximately $x - x_o = 0.5$ cm. In this case the jets are sufficiently strong to produce backflow when they penetrate to the centerline whereas, in the former case, the jets are too diffuse to produce backflow at the centerline. The two peaks for $G_r = 3.93$ correspond to the zones of maximum velocity gradients associated with the interface between the two recirculation zones. The elevated and broad peak for $G_r = 1.74$ may be attributed to the highly intermittent and dynamic coupling between the primary jets and the recirculation zone. Although the jets do not penetrate

to the core of the flow, their impact is to enhance the intermittency associated with the rear of the recirculation zone. This 'form intermittency' is additive to the true turbulence.

For $G_r = 6.99$, the solitary peak represents the point at which the jets penetrate to the centerline. The jets produce sufficient momentum in this case to 'feed' the recirculation zone and hence only one zone of recirculation is produced.

Smaller peaks detected at $x - x_o = 8$, correspond to the axial location of the dilution jets. For $G_r = 6.99$, the dilution jets do not penetrate as shown by the absence of an increase in turbulence production.

The curves for Module 2 show similar trends. For $G_r = 1.74$, the two peaks in turbulence intensity correspond to the regime (Regime III) noted in Module 1 for $G_r = 3.93$. For $G_r = 3.93$ in Module 2, the single peak is indicative of Regime IV where the primary jets 'feed' the recirculation zone ($G_r = 6.99$ in Module 1).

The flow contribution from the primary jets into the dome region was calculated based on radial profiles of axial velocity profiles 2 cm upstream of the primary jets ($x - x_o = -2$). Density was calculated based on an ideal gas assumption using measured mean temperatures. The results show that the absolute mass recirculated increases with G_r in both modules. The percent mass contributed, m_r, was calculated from the ratio of the mass flowing back into the primary zone to the sum of the incoming swirl and primary jet mass flow: $m_r = m_{bf}/(m_{pj} + m_s)$. In Module 1, $m_r = 1.2$, 2.2, and 10.8 percent for $G_r = 1.74$, 3.93, and 6.99 respectively. In Module 2 for $G_r = 3.93$, $m_r = 18.6\%$, almost an order of magnitude compared to that in Module 1. As demonstrated in the velocity and rms plots, the transition between regimes occurs at lower G_r in Module 2; that is, for $G_r = 3.93$ the flow is in Regime III in Module 1 whereas in Module 2 it is still in Regime IV.

Thermal Field:

Mean temperature profiles obtained in the plane of symmetry between the jets in Module 1 are shown in Fig. 3. Note that in this figure and other temperature field plots, the half plane from the centerline to the wall is presented. (In Fig. 3, the wall is at the top of each field plot.) For each condition, a cold region occurs at the front corner of the combustor. This is a zone of recirculation associated with the step expansion from the swirler to the duct and, because of the heat sink provided by the wall (and likelihood of a lean mixture as well), a reaction cannot be sustained. By defining x_p to be the position
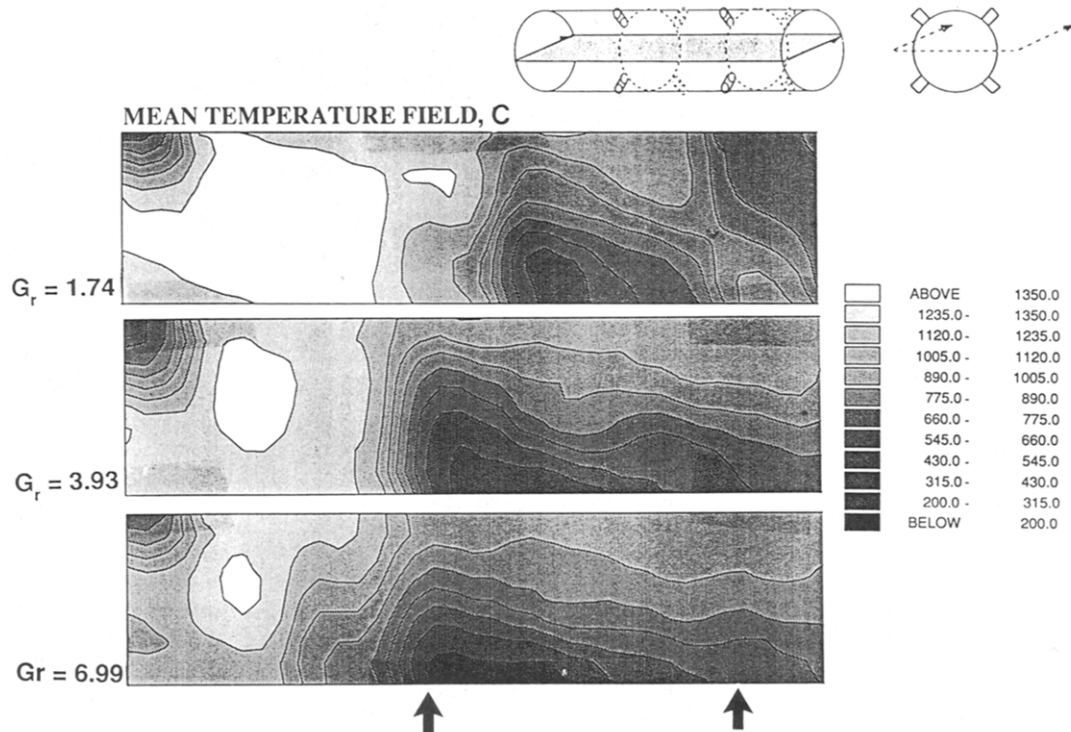

FIG. 3. The mean temperature field in the plane of symmetry between the jets for Module 1.
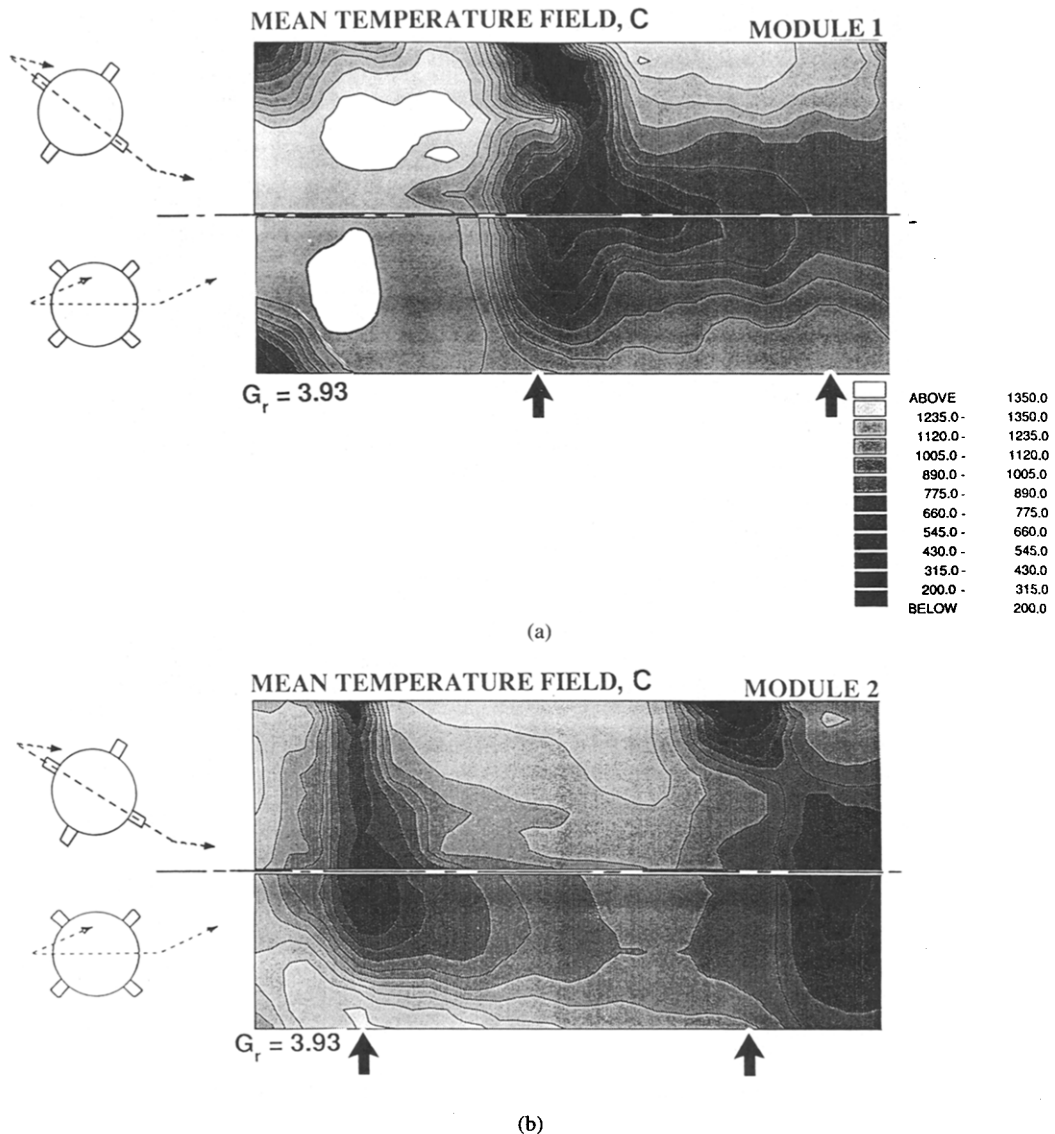
MEAN TEMPERATURE FIELD, C   MODULE 1

$G_r = 3.93$

	ABOVE	1350.0
	1235.0 -	1350.0
	1120.0 -	1235.0
	1005.0 -	1120.0
	890.0 -	1005.0
	775.0 -	890.0
	660.0 -	775.0
	545.0 -	660.0
	430.0 -	545.0
	315.0 -	430.0
	200.0 -	315.0
	BELOW	200.0

(a)

MEAN TEMPERATURE FIELD, C   MODULE 2

$G_r = 3.93$

(b)

FIG. 4. A comparison of the mean temperature fields in Modules 1 and 2. a) A two plane view of the mean temperature field in Module 1. b) A two plane view of the mean temperature field in Module 2.

corresponding to the minimum centerline temperature, the x_p are 10, 9, and 8 cm respectively for G_r increasing from 1.74 to 6.99. The influence of increasing jet momentum can be detected as well in the increasing size of regions of reduced temperature along the centerline.

In Fig. 4a, a view of temperature contours obtained in the plane of symmetry *through the jets* is shown in conjunction with contours obtained in the plane of symmetry *between the jets*. The trajectory of the jets is evident, and the containment of the dome region reaction by the penetration of the primary jets to the centerline can be clearly deduced. The hot gases in the dome region move around the

jets and are directed towards the wall in the secondary region between the jets as a result of the cold core produced by the jets. The dilution jets are seen to be more diffuse in character. This illustrates the strong three dimensionality of the flow in the vicinity of the jets and downstream of the jets. In contrast, a major portion of the dome region is nearly axisymmetric. First, the corner expansion is axisymmetric. Second, the hot torroidal region can also be seen in both plots with symmetry in the upstream core.

The hot torroidal zone is present for $G_r = 6.99$ (Fig. 3) as well as $G_r = 3.93$. For $G_r = 1.74$, the hot zone has extended to the centerline, forming

an on-axis hot zone. This is a consequence of the relatively small contribution of air from the primary jets. Recall that the equivalence ratio in the dome is unity based on the propane flow and swirl air. Thus the decreasing size of the torroidal hot zone with increasing momentum ratio is a consequence of increasingly lean combustion and the introduction of cold air along the centerline.

Fig. 4b shows a similar view of the temperature field in Module 2 for $G_r = 3.93$. The influence of the jets on the dome structure is clearly evident. The hot torroidal zone present in Module 1 is absent, temperatures are substantially reduced, and axisymmetric features in the dome have been eliminated. The jets in this case dominate the dome structure.

Emissions:

For all the conditions considered, CO levels were low (<1000 ppm) indicating efficient overall combustion. CO and NO_x emissions were spatially depressed at the centerline and increased towards the wall. O_2 profiles exhibit the reverse behavior. Major differences between emissions from Module 1 and 2 were not observed. This is most likely due to effective dome region mixing between the gaseous fuel and air. In a parallel study, in which a liquid fuel (JP-4) was used in the two modules, significant differences were observed in the emissions from the two modules with a relatively lower overall combustion efficiency in Module 2.[10]

Conclusions

This investigation reveals the importance and the complexities associated with the primary jets in controlling combustor aerothermal behavior and the overall performance. The momentum flux ratio between the primary jets and swirl air has been considered as well as the relative position of the primary jets to the swirl injection plane.

The following conclusions are drawn from this study:

• Four regimes, differentiated by the extent of primary jet penetration and resulting aerodynamic structure, have been identified to describe the influence of jet-to-swirl momentum ratio on a model can combustor.

• While the dome region displays zones of axisymmetry, the flow in the near vicinity and wake of the primary jets is highly three-dimensional.

• For the present geometry and flow conditions, the placement of the primary jets 1/2 duct diameter downstream of the inlet plane is disruptive to the formation of the swirl-induced recirculation zone. Primary jet injection and one

duct diameter downstream of the inlet plane resulted in a better match between the swirl-induced recirculation zone and the primary jets. This suggests that an optimum injection point lies somewhere in between.

While these results demonstrate and quantify the influence of jet penetration and provide a data base for industrial design codes, a fully representative simulation of actual combustors must include as well air preheat, elevated pressure, and plenum fed wall jets including possible nonuniformity between individual jet momenta.

REFERENCES

1. BRUM, R. D., AND SAMUELSEN, G. S.: Experiments in fluids, 5, 95 (1987).
2. GOULDIN, F. C., DEPSKY, J. S., AND LEE, S. L.: AIAA Journal, 23, 95 (1985).
3. LILLEY, D. G.: Investigations of Flowfields Found in Typical Combustor Geometries, NASA Contractor Report 3869, 1985.
4. BICEN, A. F., AND JONES, W. P.: Comb. Sci. Tech., 49, 1 (1986).
5. HEITOR, M. V. AND WHITELAW, J. H.: Comb. Flame, 64, 1 (1986).
6. CAMERON, C. D., BROUWER, J., SAMUELSEN, G. S.: Twenty Second Symposium (International) on Combustion. p. 465, The Combustion Institute, 1989.
7. CAMERON, C. D., BROUWER, J., SAMUELSEN, G. S.: Eng. for Gas Turbines and Power, 111, (1989).
8. RICHARDS, C. D.: An Investigation of Opposed Radial Jets with a Confined Duct Flow, Ph.D. Dissertation, UCI Combustion Laboratory Technical Report ARTR 90-6, University of California, Irvine, CA, 92717, 1990.
9. MCMURRY, C. B. AND LILLEY, D. G.: Experiments on Two Opposed Lateral Jets Injected into a Swirling Crossflow, NASA Report 175041, 1986.
10. RICHARDS, C. D. AND SAMUELSEN, G. S.: Eng. for Gas Turbines and Power, (1990).